AIAA JOURNAL
Vol. 33, No. 11, November 1995

Three-Dimensional Boundary-Layer Transition on a Swept Wing at Mach 3.5

L. N. Cattafesta III*
High Technology Corporation, Hampton, Virginia 23666
V. Iyer†
ViGYAN, Inc., Hampton, Virginia 23666
J. A. Masad‡
High Technology Corporation, Hampton, Virginia 23666
and
R. A. King§ and J. R. Dagenhart§
NASA Langley Research Center, Hampton, Virginia 23681-0001

Transition on a swept-wing leading-edge model at Mach 3.5 is investigated. Surface pressure and temperature measurements are obtained in the NASA Langley Research Center Supersonic Low-Disturbance Tunnel. For one case, temperature-sensitive paint and a sublimating chemical are used to visualize surface flow features such as transition location. The experimental data are compared with 1) mean-flow results computed as solutions to the thin-layer Navier–Stokes equations and 2) N-factors obtained using the envelope e^N method. The experimental and computational results compare favorably in most cases. In particular, $N \cong 13$ correlates best with the observed transition location over a range of freestream unit Reynolds numbers and angles of attack. Computed traveling crossflow disturbances with frequencies of 40–60 kHz have the largest N factors, and the surface flow visualizations reveal smooth transition fronts with only faint evidence of stationary crossflow vortices. These results suggest that transition is probably dominated by traveling, rather than stationary, crossflow disturbances for the present model.

Introduction

LAMINAR flow control (LFC) has the potential for achieving significant fuel savings in future supersonic transports, such as the proposed high-speed civil transport.[1] However, numerous technical challenges are associated with achieving laminar flow over a significant portion of a highly swept supersonic wing. Among these challenges is the need to predict and control the amplification of disturbances in the boundary layer. These disturbances take the form of various instability waves in a supersonic swept-wing boundary layer: Tollmien–Schlichting (TS), crossflow, and Görtler disturbances. The amplification of these disturbances leads to transition, the exact location of which is a function of wing geometry, angle of attack, Reynolds number, Mach number, background disturbance environment, surface roughness, etc. Furthermore, the incorporation of LFC via suction involves additional parameters such as suction rate and its distribution over the wing surface.

Successful implementation of LFC requires that reliable methods first be developed for predicting boundary-layer transition and quantifying its sensitivity to various parameters.[2] The aircraft industry commonly employs transition-prediction methods that are based on simple correlations (e.g., maximum values for momentum thickness and crossflow Reynolds number). A more reliable method employs linear stability theory via the e^N method, in which correlations are obtained between computed disturbance amplification factors N and measured transition locations on smooth models in low background disturbance (i.e., quiet) wind tunnels.[3] This method is capable of providing useful information on effects such as angle of attack, Reynolds number, and suction level. However, the method cannot account for other important factors in the transition process such as receptivity and nonlinear interactions. Hence, it falls short of more advanced prediction tools using the parabolized stability equations (PSE) and direct numerical simulations (DNS).[4–6] Nonetheless, the e^N method represents the state-of-the-art transition-prediction technique.

Iyer et al.[7] point out that most previous high-speed studies that employed the e^N method were restricted to two-dimensional, axisymmetric, or simple three-dimensional flow (e.g., an infinite swept wing or a swept tapered wing with straight isobars). These restrictions have been primarily due to two factors: the difficulty associated with obtaining the accurate mean-flow solutions necessary for meaningful stability analysis over complex geometries and the lack of experiments that involve complex geometries in low-disturbance environments. The former problem has been addressed with the development of many Navier–Stokes (NS) codes during the last decade. This development has prompted several recent assessments of the accuracy requirements for stability computations.[8–11] The latter problem has been alleviated with the advent of supersonic quiet tunnels.[12–15] Despite the recent advances in quiet tunnels, there has been very little research in these facilities on models with fully three-dimensional flow. The experiments of King on a sharp cone at angle of attack represent, to the best of our knowledge, the only other published work on high-speed three-dimensional boundary layers in a quiet wind tunnel.[16]

This paper describes a three-dimensional boundary-layer transition study on a swept wing at Mach 3.5. For the present study, experiments are performed on a swept-wing leading-edge model installed in the NASA Langley Research Center Supersonic Low-Disturbance Tunnel. Surface pressure distributions are obtained on a pressure model over a range of angles of attack α and freestream unit Reynolds numbers Re_∞. These distributions are compared with computed solutions to the compressible thin-layer NS equations.

Surface temperature distributions are obtained on a thin-skin thermocouple model. In addition, temperature-sensitive paint and sublimating chemical techniques are used to visualize the transition

Presented as Paper 94-2375 at the AIAA 25th Fluid Dynamics Conference, Colorado Springs, CO, June 20–23, 1994; received July 19, 1994; revision received March 31, 1995; accepted for publication April 24, 1995.

*Research Scientist, 28 Research Drive, P.O. Box 7262. Member AIAA.
†Currently Senior Research Scientist, High Technology Corporation, Hampton, VA 23666. Senior Member AIAA.
‡Research Scientist, 28 Research Drive, P.O. Box 7262. Senior Member AIAA.
§Research Engineer, Flow Modeling and Control Branch, Fluid Mechanics and Acoustics Division. Member AIAA.

pattern for a single case. Recovery factors calculated from the thermocouple measurements are used to correlate with N-factor distributions computed with the e^N method.

It is important to note that, although the present work is limited to mean-flow measurements of surface quantities, it would be highly desirable to obtain detailed boundary-layer measurements (both of the mean flow and of the instability waves). Such measurements are difficult, even at low speeds on simple geometries,[17] and must await future work. For now, we must attempt to understand the transition process using only mean surface measurements.

The paper is organized as follows. The experimental facility, wind-tunnel models, and experimental methods are described, and the computational methods and data analyses are summarized. The experimental results and comparison with the computations are then discussed, followed by the conclusions.

Experimental Setup

Facility

The experiments are conducted in the NASA Langley Supersonic Low-Disturbance Tunnel with the Mach 3.5 two-dimensional nozzle installed.[12,13] The tunnel is a blowdown type, supplied by regulated high-pressure dry air. The tunnel is connected to large vacuum spheres, which provide essentially continuous operation. The nozzle combines a rapid-expansion contour, boundary-layer bleeds upstream of the throat, and highly polished walls to maximize the extent of laminar nozzle-wall boundary layers downstream of the throat.

As shown in Fig. 1, a quiet test core in the upstream part of the uniform Mach 3.5 test rhombus is obtained when the boundary-layer bleeds are open. The extent of this quiet test core depends upon Re_∞; the larger regions of quiet flow are associated with the lower values of Re_∞. When the boundary-layer bleeds are closed (to emulate a conventional supersonic nozzle), transition of the nozzle-wall boundary layers moves upstream. Under the closed bleed-valve condition, the nozzle-wall boundary layers are completely turbulent at all but the lowest values of Re_∞. Turbulent nozzle-wall boundary layers increase the freestream noise level because of the propagation of acoustic energy along the Mach lines that emanate from turbulent eddies in the boundary layer.

Swept-Wing Leading-Edge Models

The model geometry corresponds to a symmetric representation of the first 6.25% chord region of a highly swept supersonic wing. The lateral sections of the model normal to the leading edge consist of a fixed cross section. (See Ref. 7 for more details.) The model is 38.1 cm long, measured axially from apex to base. The leading-edge sweep angle is 77.1 deg, which results in a normal Mach number of 0.78.

The experiments utilize two models with nominally identical external shapes. One model has 47 pressure taps (0.508 mm OD/0.254 mm ID). Seventeen taps are located at the $x = 12.7$ cm station, and the other 30 taps are located at the $x = 25.4$ cm station. A second thin-skin model (0.762 mm thick) is instrumented with 231 type-K thermocouples welded to the skin interior. The nominal surface finish of the thermocouple model is 0.1 μm rms, and that of the pressure model is 0.4 μm rms. The geometry of both models was also checked using a computer-controlled probe at the $x = 6.35$, 12.7, 19.05, 25.4, and 31.75 cm axial locations. For the pressure model, the maximum observed error (from the entire data set) is 0.23 mm, and the 2σ value of the error distribution is 0.09 mm. The corresponding maximum error and 2σ value for the thermocouple model are 0.2 and 0.11 mm, respectively.

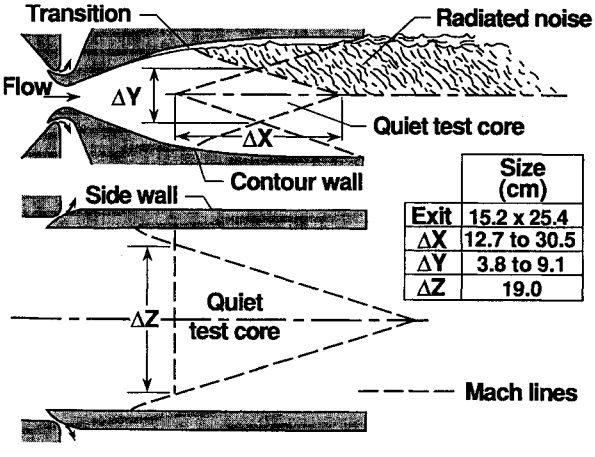

Fig. 1 Quiet test core in Mach 3.5 two-dimensional nozzle.

Surface Flow Visualization Methods

In addition to surface pressure and temperature measurements, various surface flow visualization techniques are employed. These include oil flow visualization,[18] the sublimating chemical method,[18] and temperature-sensitive paint (TSP).[19] (See the indicated references for details.) Each of these methods complements the quantitative surface measurements. For example, the oil flow technique is used to examine surface streamline patterns and identifies vortex tracks and regions of separated flow. For these experiments, a 3:1 mixture by volume of 200 cS silicon oil and titanium dioxide powder is used.

In its simplest form, used here, TSP provides a global image of the wall temperature distribution. This method is capable of providing far greater spatial resolution than is possible with thermocouple measurements. Furthermore, TSP can provide quantitative information, as explained by Donovan et al.[19] In the present experiments, TSP is used to visualize the transition location for a single case, which is then compared with that determined with thermocouples. (The thermocouple transition criterion is described later.)

The sublimating chemical technique is also extremely useful for determining surface flow patterns. In the present experiments, the chemical fluorene (i.e., $C_{13}H_{10}$) is dissolved in ethyl alcohol to provide a saturated solution and is then sprayed on the surface of the thermocouple model with a touch-up gun. The alcohol evaporates during this process, which leaves the fluorene on the model surface. This chemical sublimes at a rate that is directly related to the local surface shear stress. Thus, the technique is capable of identifying both the transition location and stationary crossflow disturbances, although care must be exercised in interpreting the resulting patterns due to time-history effects, nonuniform surface coatings, and artificial roughness introduced by the coating. This technique is used to visualize the same case examined with TSP and provides an additional assessment of the thermocouple method.

Test Conditions

The wind-tunnel tests are conducted in both noisy and quiet freestream conditions, although only the quiet data are discussed here. The tunnel stagnation temperature is set at approximately

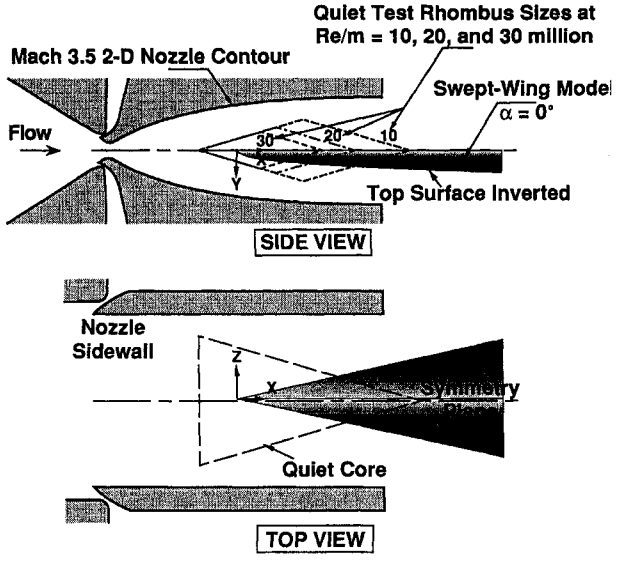

Fig. 2 Swept-wing leading-edge model.

333 K, which results in model recovery temperatures that roughly match pretest model temperatures. Because of the thermocouple model's thin skin (0.762 mm), the temperature data are obtained under nearly adiabatic wall conditions. The Re_∞ is varied from 5 to 26×10^6/m by varying the tunnel stagnation pressure from 0.1 to 0.59 MPa (±6.9 kPa), and α is also varied from −2 to 5 deg (±0.1 deg) in 1-deg increments. Note that α is defined in the conventional sense as the angle in the x–y plane between the freestream velocity vector and the x axis (Fig. 2). The angle of yaw is maintained below 0.05 deg.

The model is mounted inverted with its symmetry plane displaced +3.175 mm from the nozzle x–y plane and its apex located 18.25 cm downstream of the nozzle throat, as shown in Fig. 2. This placement ensures that the model apex is always contained within the Mach 3.5 test rhombus and accommodates existing model-mounting constraints. The angle of attack is adjusted by rotating the model in the x–y plane about a pivot point that is 45.72 cm from the model apex. The extent of the model contained in the quiet core is depicted in the figure for three different values of Re_∞ at $\alpha = 0$ deg.

Computational Methods and Data Analyses

A crucial part of any stability computation is the accurate determination of the mean flow. In the present case, the flow is significantly three dimensional; in addition, the short length of the model precludes the assumption of a fully developed infinite swept-wing flow.

Therefore, the mean flow is obtained by solving the compressible, three-dimensional, thin-layer NS equations. A finite volume upwind-differenced NS solver (CFL3D) has been employed for this purpose.[20] This code has been used extensively by various researchers for accurate flow calculations that range from subsonic to hypersonic Mach numbers. Mean-flow solutions are calculated in terms of Cartesian velocities, temperature, and density profiles on a general curvilinear grid. Details of the application of this code to the present geometry as well as to the development of an interface program for the purpose of stability calculations are provided in previous publications.[7,8,21]

In the present work, the calculations have been repeated for several conditions. For the results presented here, the grid in the normal direction consists of 121 points (compared with 61 in previous work). This number provides adequate resolution of the mean-flow solution profiles normal to the wall with approximately 70 points in the boundary layer.

The stability analysis of the computed mean-flow profiles is performed with the computer code COSAL, which is modified for fully three-dimensional flow.[7,22] In particular, temporal stability calculations are performed with the envelope method (in which the real frequency of the disturbances is specified and the temporal growth rate is maximized with respect to wave orientation). The frequency range of the disturbances in the present calculations is varied from 0 to 70 kHz. To compute the N factor, a spatial growth rate is obtained using the Gaster transformation by dividing the temporal growth rate by the real part of the group velocity. The resulting spatial growth rate is then integrated along the curve whose tangent is defined by the real part of the group velocity vector.

The stability calculations invoke the quasiparallel flow assumption and also neglect the effect of body curvature. For supersonic flow over a finite swept wing, the repercussions of these assumptions are not known at present. However, for low-speed flow over an infinite swept cylinder, body curvature has a stabilizing effect, whereas nonparallelism is destabilizing.[23–26] The destabilizing effect of nonparallel flow has also been demonstrated for incompressible flow over an infinite swept cylinder using the linear parabolized stability equations (linear PSE).[27]

It should also be noted that, at the test Mach number of 3.5 and nearly adiabatic wall conditions, the second mode of instability is damped and, therefore, does not contribute to the transition process.[28] Thus, any TS wave contributions to transition in the regions of small crossflow are due to the first mode of instability.

The procedure for correlating the observed transition location and computed N factors is as follows. The only quantitative measurement of the transition location available for all test cases is obtained from the steady-state wall temperature distribution, which is measured with thermocouples. The present method represents an

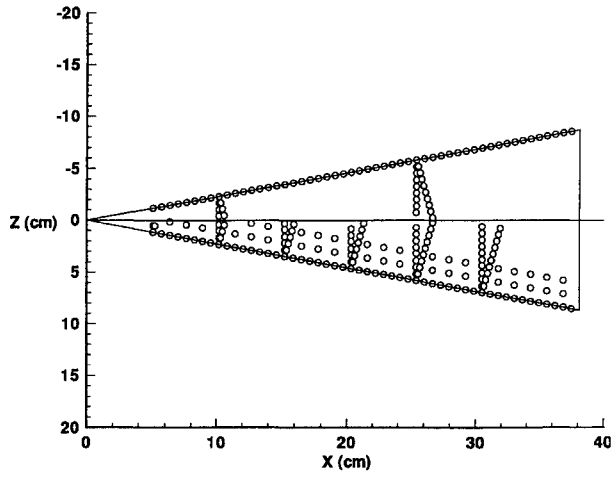

Fig. 3 Thermocouple locations on swept-wing leading-edge model.

extension of the transient thermocouple method for thin-skin models to a steady-state condition.[29] The transient method equates the convective heat transfer rate to the rate of change of energy contained within a volume. At steady state, the skin achieves adiabatic conditions, if conduction and radiation effects are negligible. These assumptions are reasonable for the thermocouple model except near the base of the model.

The locations of these measurements on the upper surface of the model are shown in Fig. 3. Rows of thermocouples are located parallel to the leading edge, along lines normal to the leading edge, and at constant x locations. The more densely instrumented half of the model contains 156 of the 231 thermocouples, and this side is used in the correlation. Despite this seemingly large number of thermocouples, adequate resolution of the transition location for all of the test cases is not possible. This limitation is a drawback of the present method and emphasizes the need for higher spatial-resolution transition-location measurement techniques for three-dimensional flows.

With the standard definition, a recovery factor is calculated based on the ratio of the measured wall temperature to the measured tunnel stagnation temperature, T_w/T_t, and the computed ratio of the boundary-layer edge temperature to the stagnation temperature, T_e/T_t:

$$r = \frac{T_w - T_e}{T_t - T_e} = \frac{(T_w/T_t) - (T_e/T_t)}{1 - (T_e/T_t)} \tag{1}$$

The calculated recovery factors at the discrete measurement locations are then interpolated to the structured surface grid used in the computation. In all of the examined cases, r ranged from approximately 0.85 to 0.88, values typical of laminar and turbulent flow, respectively. Transition appears as a region of high gradients in a contour plot of recovery factor, although it is difficult to determine precisely where transition begins. This is because the transition fronts are three dimensional and are not always resolved well. Hence, for a single case ($Re_\infty = 13.8 \times 10^6$/m and $\alpha = -2$ deg), the transition location is determined by correlating a recovery factor range with the transition location obtained using the sublimating chemical fluorene and temperature-sensitive paint.[18,19] The resulting transition front locations obtained using these latter two methods agreed quite well with each other and correlated best with the range $r = 0.865 \pm 0.002$. For all other cases, then, this criterion is used to determine the transition location. Although this criterion may not correspond exactly to the beginning of transition, a visual inspection of r contour plots shows that it does represent the first clear increase in r above laminar values.

It should be emphasized that because T_e varies over the model (due to the three-dimensional flow) and is not measured, the computed value of T_e/T_t is needed to calculate r correctly. This ratio is an inviscid quantity and, hence, introduces negligible uncertainty into the calculation of r compared with that introduced by T_w/T_t. A conventional root-sum-square uncertainty analysis thus provides an uncertainty estimate for r of ±0.002 (using typical values in the

transition region and 95% uncertainty estimates of ±0.4 K for T_w and T_t). Several tests completed at random over a period of two years for a single case ($Re_\infty = 13.8 \times 10^6$/m and $\alpha = -2$ deg) have shown that the results are extremely repeatable, such that the preceding uncertainty estimate encompasses the observed scatter in the data.

Results and Discussion

Comparison of C_p Distributions

As a first step in the process of correlating computational and experimental results, the pressure coefficient C_p values are compared. From the large database of experimental measurements, a few cases are selected for comparison. Figure 4 represents a typical comparison. Note that the computation assumes fully laminar flow over the model and also uses an adiabatic wall boundary condition—instead of, for example, the measured wall temperature distribution.

Figure 4 shows the variation of C_p at the $x = 25.4$ cm cross section normal to the symmetry plane for a) $\alpha = 0$ deg and $Re_\infty = 7.9 \times 10^6$/m and b) $\alpha = 3$ deg and $Re_\infty = 7.9 \times 10^6$/m. The experimental data points correspond to two unit Reynolds numbers close to that of the calculation. The typical uncertainty in C_p is approximately ±0.003; the actual value is shown in the figure. The pressure distributions on the upper surface exhibit the strong accelerations in the vicinity of the swept leading edge that are typical of crossflow-dominated regions.

Although the overall comparison is good, some differences do exist in a few cases. Figure 5 represents the case with the largest observed disagreement ($\alpha = -2$ deg and $Re_\infty = 8.9 \times 10^6$/m). As an independent check on the computational result, the mean flow is also calculated with a central-differenced NS code called TLNS3D-MB.[30] The results from this calculation are included in Fig. 5. The two calculations agree on the upper surface of the model but are both shifted from the measured C_p. (The C_p distributions

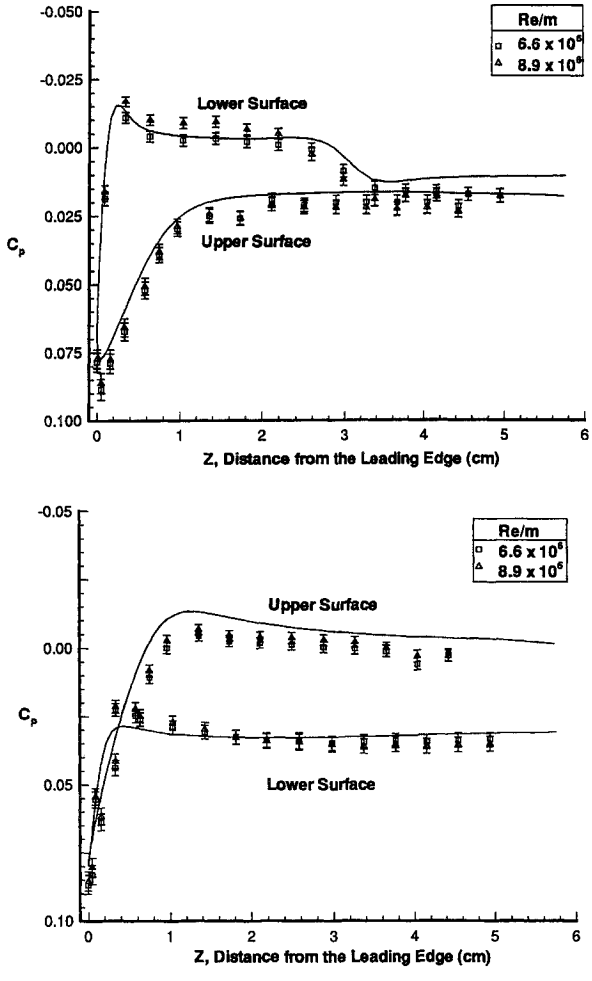

Fig. 4 Pressure coefficient C_p: a) $\alpha = 0$ deg and $Re_\infty = 7.9 \times 10^6$/m and b) $\alpha = 3$ deg and $Re_\infty = 7.9 \times 10^6$/m.

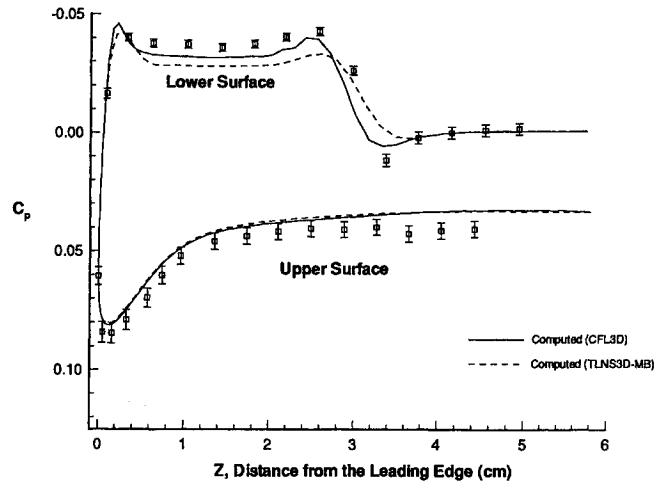

Fig. 5 Pressure coefficient C_p for $\alpha = -2$ deg and $Re_\infty = 8.9 \times 10^6$/m.

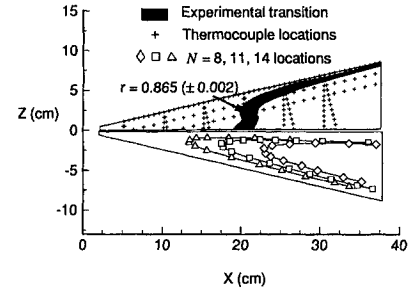

Fig. 6 Transition correlation for $\alpha = -2$ deg and $Re_\infty = 13.8 \times 10^6$/m.

computed on the lower surface show some differences, possibly because of the presence of a vortex emanating from the vicinity of the apex of the model, detected using oil flow visualization.) Although the reason for the difference between the computational and experimental results is difficult to ascertain, we believe that the source of the discrepancy arises from a slight shift in α (to more negative values) due to model deflections from the negative lift.

Note that the discrepancy discussed earlier represents the worst case. The mean-flow computations reproduce the experimental results reasonably well in all other cases examined. Unfortunately, these pressure measurements represent the only basis for comparison because no other measurements of the boundary layer have been attempted. Such boundary-layer measurements, although difficult, would of course represent a harsher test of the computations.

Transition-Location Correlation

With the computed solutions serving as the basic state for the stability analysis, an attempt is made to correlate the experimentally observed transition location with the computed N factors. One such comparison is shown in Fig. 6 for the case $\alpha = -2$ deg and $Re_\infty = 13.8 \times 10^6$/m. The computations cover a range of frequencies, with the cumulative maximum growth ratio peaking in the frequency range of 40–60 kHz. The loci of $N = 8$, 11, and 14 are shown on the plot, in addition to the experimentally determined transition front and the thermocouple locations.

From the figure, it appears that $N \cong 13$ correlates best with the transition location. The observed transition front parallel to the leading edge is indicative of a crossflow-dominated case and is seen in both the experimental and the computational results. These results agree except in the vicinity of the symmetry plane. The symmetry condition requires that the crossflow velocity be equal to zero there. Hence, if TS disturbances are weak, the transition front will be parallel to this line. The disagreement between the experimental and theoretical transition fronts in this region is due to the insufficient resolution of wall temperature provided by the thermocouples. This is verified in Fig. 7, in which the transition fronts obtained with both TSP (shown as temperature contours superimposed on the

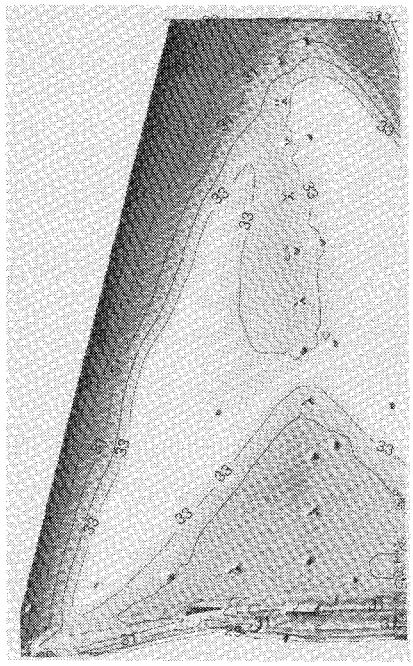

a)

b)

Fig. 7 Transition location for $\alpha = -2$ deg and $Re_\infty = 13.8 \times 10^6$/m obtained with different methods: a) temperature-sensitive paint. Temperature contours (labeled in °C) are superimposed on the temperature image. The X and O registration marks in the image denote known locations along the symmetry plane and base of the model. b) The sublimating chemical fluorene. Flow is from top to bottom in both images.

temperature greyscale image) and the sublimating chemical technique exhibit a shape like that of the N-factor loci in Fig. 6. Despite the poor resolution of the thermocouple data near the symmetry plane, a useful transition correlation can still be obtained with the thermocouple data if we ignore this region. Sufficient resolution exists in the thermocouple data to resolve the transition region elsewhere. Therefore, the effects of two parameters (i.e., Re_∞ and α) on transition location are studied.

In particular, the effect of varying Re_∞ while keeping α fixed at 0 deg is first examined. The corresponding mean-flow solutions and N factors are computed and compared with the experimental results. As shown in Fig. 8, the transition-front locations (obtained with the recovery factor criterion cited earlier) for different values of Re_∞ are plotted on the upper half of the model. In addition, the most upstream $N = 13$ locations (which correspond to those frequencies that have the largest growth ratios) are displayed on the bottom half of the model. If we ignore the symmetry-plane region, the experimental

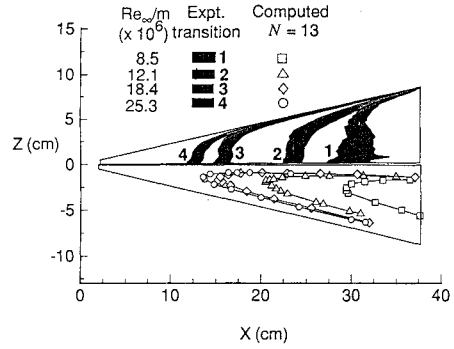

Fig. 8 Parametric variation of transition location with Re_∞ for $\alpha = 0$ deg.

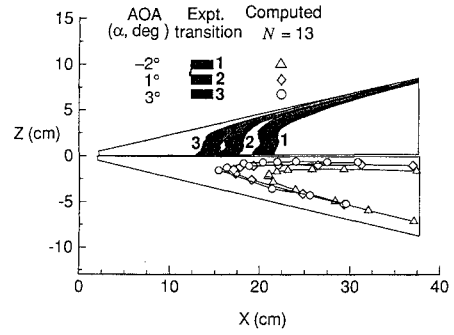

Fig. 9 Parametric variation of transition location with α for $Re_\infty \cong 13.8 \times 10^6$/m.

and the computational results show similar trends with respect to the upstream movement of the transition front as Re_∞ increases. The only region in which a discrepancy exists is close to the base of the model. This situation occurs at low unit Reynolds numbers, where disturbance growth rates are lower than at larger Re_∞, and the transition process is presumably more drawn out. Furthermore, the region near the base of the model lies outside the quiet test core (see Fig. 2) and is also susceptible to conduction effects due to the presence of internal structural members in this vicinity.

The effect of varying the angle of attack from $\alpha = -2$ to 5 deg is also studied for a constant Re_∞ of 13.8×10^6/m. The experimental transition fronts and computed $N = 13$ locations are shown in Fig. 9. As α is varied from -2 to 3 deg, both the computational and the experimental results show that transition moves forward. However, the upstream movement saturates for $\alpha = 5$ deg in the computation, whereas the experiment shows continued upstream movement of the front. (The $\alpha = 5$ deg case is not shown for clarity.) Surface oil flow visualizations of the $\alpha = 5$ deg case revealed a laminar separation bubble caused by a vortex emanating from the apex region on the upper surface, a feature not captured by the computation. This phenomenon may have caused premature transition and, hence, the resulting discrepancy.

Surface Flow Visualization

The computational results indicate that the most amplified disturbances are traveling disturbances rather than stationary disturbances. Furthermore, the fact that a good correlation exists between the $N = 13$ locations for traveling waves and the observed transition location over the parameter range examined suggests that transition on the model is dominated by traveling crossflow disturbances. This scenario contrasts with the results of low-speed experiments on swept wings by Dagenhart,[31] in which stationary crossflow disturbances dominate the transition process even though they are less amplified (presumably because they have large initial amplitudes due to surface roughness effects). Surface flow visualizations of transition in the study of Dagenhart show distinct jagged or sawtooth patterns in the transition fronts. Other studies by Poll[32] and Takagi and Itoh[33] in the crossflow region on yawed circular cylinders show strong evidence that traveling waves dominate the transition process.

The case with $\alpha = -2$ deg and $Re_\infty \approx 13.8 \times 10^6$/m is thus examined using the sublimating chemical technique with fluorene.

Figure 7b, shown earlier, displays the resulting pattern for the aforementioned case. Although streaks produced by stationary crossflow vortices are present (measured spacing/computed local boundary layer thickness ≈2), they do not produce a sawtooth transition pattern as in the low-speed case studied by Dagenhart. Indeed, repeated tests sometimes display the pattern reproduced in the figure but often reveal little or no evidence of stationary vortices. Only when roughness elements (taking the form of nominally 2.5-μm-thick, 2.54-mm-diam rub-on dots) are placed on the model surface near the model leading edge does the stationary pattern always appear. These facts demonstrate the sensitivity of the method to the random surface roughness introduced by the coating and, furthermore, emphasize the need for care in interpreting the results. Clearly, boundary-layer disturbance measurements are highly desirable.

Nonetheless, the transition front location is quite repeatable when no roughness is intentionally added, independent of the appearance of stationary disturbances. The addition of roughness elements, on the other hand, can shift the transition location further upstream. Based on these observations, it appears reasonable to conclude that the transition process on the smooth surface is dominated by traveling disturbances.

Conclusions

An experimental study of transition on a swept-wing leading-edge model has been conducted in the NASA Langley Research Center Supersonic Low-Disturbance Tunnel at Mach 3.5. In particular, C_p distributions and transition-location measurements have been obtained from pressure and wall temperature measurements on pressure and thin-skin thermocouple models, respectively. Sublimating chemical surface flow visualization has also been used to investigate the stationary disturbance pattern. Temperature-sensitive paint has been successfully employed to obtain a global surface-temperature distribution for a single case. The results exhibit sharp pressure gradients in the vicinity of the leading edge and transition fronts that are approximately parallel to the leading edge, both of which are characteristic features of a crossflow-dominated transition process. The surface flow visualization results demonstrate that a clean model surface shows faint evidence of stationary disturbances and a fairly smooth transition front, in which case the traveling crossflow disturbances likely play a major role in the transition process.

Mean-flow Navier–Stokes solutions have been obtained with CFL3D, a finite volume upwind-difference code. These solutions, which compare favorably with measured C_p distributions for most cases, have served as input to linear stability calculations using the envelope e^N method. The N factors have been calculated and compared with the observed transition locations. In particular, traveling disturbances with $N \cong 13$ provide a good correlation with the transition data over a range of unit Reynolds numbers and angles of attack.

Acknowledgments

The first author gratefully acknowledges the support received from the Experimental Flow Physics Branch of the Fluid Mechanics Division, NASA Langley Research Center, Contract NAS1-18585. The second and third authors gratefully acknowledge the support received from the Theoretical Flow Physics Branch of the Fluid Mechanics Division, NASA Langley Research Center, Contracts NAS1-19672 and NAS1-19299, respectively.

References

[1]Hefner, J. N., and Sabo, F. E., "Research in Natural Laminar Flow and Laminar-Flow Control," NASA CP 2487, Pt. 1, March 1987.

[2]Malik, M. R., "Stability Theory for Laminar Flow Control Design," *Viscous Drag Reduction in Boundary Layers*, Vol. 123, Progress in Astronautics and Aeronautics, AIAA, Washington, DC, 1990, pp. 3–46.

[3]Bushnell, D. M., Malik, M. R., and Harvey, W., "Transition Prediction in External Flows with Linear Stability Theory," *IUTAM Symposium Transsonicum III*, Springer–Verlag, Berlin, 1988, pp. 225–242.

[4]Bertolotti, F. P., and Herbert, T., "Analysis of the Linear Stability of Compressible Boundary Layers Using the PSE," *Theoretical and Computational Fluid Dynamics*, Vol. 3, 1991, pp. 117–124.

[5]Chang, C.-L., Malik, M. R., Erlebacher, G., and Hussaini, M. Y., "Compressible Stability of Growing Boundary Layers Using Parabolized Stability Equations," AIAA Paper 91-1636, June 1991.

[6]Pruett, C. D., and Chang, C.-L., "A Comparison of PSE and DNS for High-Speed Boundary-Layer Flows," *Symposium of Transitional and Turbulent Compressible Flows*, FED-Vol. 151, American Society of Mechanical Engineers, New York, 1993, pp. 57–67.

[7]Iyer, V., Spall, R., and Dagenhart, J., "Computational Study of Transition Front on a Swept Wing Leading-Edge Model," *Journal of Aircraft*, Vol. 31, No. 1, 1994, pp. 72–78.

[8]Iyer, V., "Assessment of Meanflow Solutions for Instability Analysis of Transitioning Flows," AIAA Paper 91-1638, June 1991.

[9]Ramakrishnan, R., Vatsa, V., Otto, J., and Kumar, A., "A Detailed Study of Mean-Flow Solutions for Stability of Transitional Flows," AIAA Paper 93-3052, July 1993.

[10]Garriz, J. A., Vatsa, V., and Sanetrik, M. D., "Issues Involved in Coupling Navier–Stokes Mean-Flow and Linear Stability Codes," AIAA Paper 94-0304, Jan. 1994.

[11]Kufner, E., Dallmann, U., and Stilla, J., "Instability of Hypersonic Flow Past Blunt Cones—Effects of Mean Flow Variations," AIAA Paper 93-2983, July 1993.

[12]Beckwith, I. E., Creel, T. R., Jr., Chen, F.-J., and Kendall, J. M., "Freestream Noise and Transition Measurements in a Mach 3.5 Pilot Quiet Tunnel," AIAA Paper 83-0042, Jan. 1983.

[13]Beckwith, I. E., and Miller, C. G., III, "Aerothermodynamics and Transition in High-Speed Wind Tunnels at NASA Langley," *Annual Review of Fluid Mechanics*, Vol. 22, 1990, pp. 419–439.

[14]Wolf, S. W. D., Laub, J. A., and King, L. S., "Flow Characteristics of the NASA-Ames Laminar Flow Supersonic Wind Tunnel for Mach 1.6 Operation," AIAA Paper 94-2502, June 1994.

[15]Schneider, S. P., and Haven, C. E., "Quiet-Flow Ludwieg Tube for High-Speed Transition Research," *AIAA Journal*, Vol. 33, No. 4, 1995, pp. 688–693.

[16]King, R. A., "Three-Dimensional Boundary-Layer Transition on a Cone at Mach 3.5," *Experiments in Fluids*, Vol. 13, 1992, pp. 305–314.

[17]Saric, W., "Low-Speed Boundary-Layer Transition Experiments," ICASE/NASA LaRC Short Course on Transition, Hampton, VA, June 1993.

[18]Obara, C. J., "Sublimating Chemical Technique for Boundary-Layer Flow Visualization in Flight Testing," *Journal of Aircraft*, Vol. 25, No. 6, 1988, pp. 493–498.

[19]Donovan, J. F., Morris, M. J., Pal, A., Benne, M. E., and Crites, R. C., "Data Analysis Techniques for Pressure and Temperature-Sensitive Paints," AIAA Paper 93-0176, Jan. 1993.

[20]Thomas, J., Taylor, S., and Anderson, W., "Navier–Stokes Computations of Vortical Flows over Low Aspect Ratio Wings," AIAA Paper 87-0207, Jan. 1987.

[21]Iyer, V., and Spall, R., "Application of Linear Stability Theory in Laminar Flow Design," Society of Automotive Engineers, SAE Paper 912116, Sept. 1991.

[22]Malik, M. R., "COSAL—A Black Box Compressible Stability Code for Three-Dimensional Boundary Layers," NASA CR-165925, 1982.

[23]Malik, M. R., and Balakumar, P., "Linear Stability of Three-Dimensional Boundary Layers: Effects of Curvature and Non-Parallelism," AIAA Paper 93-0079, Jan. 1993.

[24]Masad, J. A., and Malik, M. R., "Effects of Body Curvature and Non-Parallelism on the Stability of Flow over a Swept Cylinder," *Physics of Fluids*, Vol. 6, No. 7, 1994, pp. 2363–2379.

[25]Schrauf, G., "Curvature Effects for Three-Dimensional Compressible Boundary-Layer Stability," *Z. Flugwiss Weltraumforsch*, Vol. 16, 1992, pp. 119–127.

[26]Lin, R. S., and Reed, H. L., "Effect of Curvature on Stationary Crossflow Instability of a Three-Dimensional Boundary Layer," *AIAA Journal*, Vol. 31, No. 9, 1993, pp. 1611–1617.

[27]Wang, M., Herbert, T., and Stuckert, G. K., "Crossflow-Induced Transition in Compressible Swept-Wing Flows," AIAA Paper 94-2374, June 1994.

[28]Mack, L. M., "Boundary-Layer Linear Stability Theory," AGARD Rept. 709, March 1984.

[29]Owen, F. K., Horstman, C. C., Stainback, P. C., and Wagner, R. D., "Comparison of Wind Tunnel Transition and Freestream Disturbance Measurements," *AIAA Journal*, Vol. 13, No. 3, 1975, pp. 266–269.

[30]Vatsa, V., Sanetrik, M. D., Parlette, E., Eiseman, P., and Cheng, Z., "Multi-Block Structured Grid Approach for Solving Flows over Complex Aerodynamic Configurations," AIAA Paper 94-0655, Jan. 1994.

[31]Dagenhart, J. R., "Crossflow Stability and Transition Experiments in a Swept-Wing Flow," Ph.D. Dissertation, Engineering Mechanics Dept., Virginia Polytechnic Inst. and State Univ., Blacksburg, VA, 1992; see also NASA TM-108650, 1992.

[32]Poll, D. I. A., "Some Observations of the Transition Process on the Wind-Ward Face of a Long Yawed Cylinder," *Journal of Fluid Mechanics*, Vol. 150, 1985, p. 329.

[33]Takagi, S., and Itoh, N., "Observation of Traveling Waves in the Three-Dimensional Boundary Layer along a Yawed Cylinder," *Fluid Dynamics Research*, Vol. 14, 1994, pp. 167–189.